

**Isotropic properties of the photonic band gap in quasicrystals with low-index contrast**

Priya Rose T., E. Di Gennaro, G. Abbate, and A. Andreone

*CNR-SPIN and Department of Physics, University of Naples Federico II, Napoli, Italy*

(Received 1 March 2011; revised manuscript received 9 June 2011; published 9 September 2011)

We report on the formation and development of the photonic band gap in two-dimensional 8-, 10-, and 12-fold symmetry quasicrystalline lattices of low-index contrast. Finite-size structures made of dielectric cylindrical rods were studied and measured in the microwave region, and their properties were compared with a conventional hexagonal crystal. Band-gap characteristics were investigated by changing the direction of propagation of the incident beam inside the crystal. Various angles of incidence from  $0^\circ$  to  $30^\circ$  were used to investigate the isotropic nature of the band gap. The arbitrarily high rotational symmetry of aperiodically ordered structures could be practically exploited to manufacture isotropic band-gap materials, which are perfectly suitable for hosting waveguides or cavities.

DOI: [10.1103/PhysRevB.84.125111](https://doi.org/10.1103/PhysRevB.84.125111)

PACS number(s): 42.70.Qs, 41.20.Jb, 61.44.Br

**I. INTRODUCTION**

Structures exhibiting photonic-band-gap (PBG) characteristics are useful in confining and guiding electromagnetic energy. Photonic crystals (PC's) are artificially engineered materials with spatially modulated refractive indices that are widely used for such purposes. There is a tremendous interest in studying their properties because of their potential application in design and manufacturing of new optical components and devices such as wavelength division multiplexers, switches, light-emitting diodes, and lasers.<sup>1-4</sup>

Recently, photonic quasicrystals (PQC's), which are structures lacking long-range translational order but with orientational order and higher-order rotational symmetries that are not compatible with the spatial periodicity, have also attracted attention because of their unique characteristics. PQC's have neither true periodicity nor translational symmetry, however they can exhibit symmetries that are not achievable by conventional periodic structures. These features have recently attracted a great deal of interest because of their potential impact in engineering novel optical circuits. Like photonic crystals, PQC's can demonstrate directive emission,<sup>5</sup> mode confinement,<sup>6</sup> and superlensing.<sup>7</sup>

A one-dimensional photonic band gap has been observed in dielectric multilayers stacked according to a Fibonacci series.<sup>8</sup> Dielectrics arranged according to quasiperiodic geometries such as octagonal (8-fold), decagonal (10-fold), and dodecagonal (12-fold) are shown to have a two-dimensional PBG.<sup>9-12</sup> Penrose-tiled (10-fold rotational symmetry) PQC's were the most studied structures among those presented above, and there were numerous studies about the mechanism of formation of a PBG,<sup>13</sup> optical properties, diffraction patterns,<sup>9</sup> and multiple scattering<sup>11</sup> for this geometry. An organic laser based on Penrose-tiled PQC's was also demonstrated.<sup>14</sup> The formation of a complete PBG in a 12-fold symmetric dodecagonal PQC was numerically and experimentally studied by Zoorob *et al.*<sup>15</sup>

The lack of periodicity renders the study of PQC's very complex and computationally demanding. Although some concepts developed for periodic PC's can be used for the analysis of the properties of PQC's, a rigorous extension of a Bloch-type theorem (and associated tools and concepts) does not exist. Previous methods include a supercell approach

in a plane-wave expansion technique to approximate the response of the infinite aperiodic lattice,<sup>9,10</sup> or the use of Archimedean-like tilings with properties similar to those of photonic quasicrystals.<sup>16</sup> Recently, a method was proposed for computing the spectra and the eigenstates of a PQC by directly solving Maxwell equations in a periodic unit cell of a higher-dimensional lattice.<sup>17</sup>

In the geometries mentioned above, the tiling was previously calculated by matching rules or inflation-deflation algorithms or using projection methods from a hypercubic lattice.<sup>18</sup> Well-known tilings are the octagonal Ammann-Beenker,<sup>19</sup> the decagonal Penrose,<sup>20</sup> and the dodecagonal pattern based on the Stampfli rule,<sup>21</sup> which represent the main quasiperiodic structures of the present study.

The interference patterns formed by multiple-beam interferometry provide another way to obtain highly symmetric quasicrystalline patterns.<sup>22</sup> Recently, holographic techniques based on interferential methods were used to fabricate PQC's with very high rotational symmetry, the fold being determined by the number of interfering beams. The PBG properties of 12-fold symmetric quasicrystal patterns formed by double-beam multiple exposure holography were studied theoretically by Gauthier *et al.*<sup>23</sup>

The method of single-beam computer-generated holography has also been successfully used to fabricate PQC structures with up to 23-fold rotational symmetry.<sup>24</sup> These techniques can be used to produce complicated two-dimensional geometries with ease. Very recently, a three-dimensional Penrose-type PQC fabricated through this method was also reported.<sup>25</sup> In considering holographic lithography, it is important to have geometries possessing optimum band-gap properties at low refractive index contrast. A conceivable application is the combination of this versatile technology and soft materials such as polymer-dispersed liquid crystals for the realization of large-area, high-quality, low-cost optical devices with switchable properties.<sup>26</sup>

In photonic crystals, the opening of full PBG's, that is, frequency ranges over which electromagnetic wave propagation is prohibited for all directions and polarizations, is a well-understood phenomenon, thoroughly studied during the past two decades. This is not the case for photonic quasicrystals, for which a systematic procedure for the design

of optimized structures with sizable full PBG's was only recently introduced.<sup>27</sup>

In two-dimensional structures, a full PBG for both transverse magnetic (TM,  $\mathbf{E}$  field orthogonal to the crystal plane) and transverse electric (TE,  $\mathbf{H}$  field orthogonal to the crystal plane) polarization is possible for high values of the index contrast only. Nevertheless, the minimum refractive index contrast  $\Delta n$  (Ref. 28) at which a partial band gap starts to appear, for a specifically polarized electromagnetic mode, is an important parameter for the development of photonic devices such as waveguides. This is very much dependent on the particular geometry used.

The minimum value for opening a partial band gap in a periodic (triangular) structure was calculated using a plane-wave technique by Matthews *et al.*<sup>29</sup> For the optimal configuration of dielectric circular rods in air (with a filling factor—the ratio between the total and the rods in an occupied area—of  $\eta = 0.3$ ), the critical value of the dielectric permittivity is 1.73 for the TM band gap (corresponding to  $\Delta n = 0.31$ ), and it is much larger for the TE band gap. This study should rule out any attempt to develop PBG devices based on periodic structures with a lower index contrast.

In the case of quasicrystal geometries, a novel method based on density waves was used to determine the polarized band gap for  $n$ -fold rotational symmetrical structures as a function of the index contrast.<sup>30</sup> This method works well for TM polarization only, for which the density function for the optimal configurations tends to have smoother features (on the scale of the wavelength) compared to the case of TE polarization. Quasicrystalline structures of high symmetry tend to have larger partial band gaps than the crystalline ones at low contrast, but smaller band gaps at high contrast. The sixfold (hexagonal) crystalline structure yields the largest gap for any value of the index contrast approximately higher than 1. The critical value for the optimized quasiperiodic photonic crystals is estimated to be close to  $\Delta n = 0.22$ .

Very recently, a detailed numerical study on the band-gap formation at low-index contrasts for both TE and TM polarization was carried out by Zito *et al.*<sup>31</sup> Using finite-difference time-domain (FDTD) simulations, the authors showed that, more than the degree of rotational symmetry, the difference in the tiling geometry might dramatically affect the existence and behavior of the band gap.

Another critical parameter that comes into play for the realization of devices is the isotropy of the PBG. For some applications, such as light-emitting diodes, this property may be desirable even if the size of the full gap is slightly reduced. The periodic structures with square or triangular lattices have anisotropic band-gap properties because of the anisotropy of the Brillouin zone (BZ). Significantly, optimized quasicrystal gaps are more isotropic than those of crystals, for all contrasts, due to their disallowed rotational symmetries. This is due to the fact that their effective BZ's are more circular than the BZ's of the periodic structures, which translates to reduced frequency undulations (that is, band-gap variations over the wave vector in the BZ).

Experimental investigations in this direction were performed by Bayindir *et al.*<sup>32</sup> in the microwave regime and by Hase *et al.*<sup>33</sup> in the far-infrared region, based on octagonal and Penrose quasicrystals. Both studies reported the appearance of a PBG having almost isotropic properties in aperiodic lattices consisting of dielectric rods in air and for an electric field parallel to the rods.

We present here a detailed and systematic analysis of the band-gap isotropy of photonic crystal and quasicrystal structures having low refractive index contrast and for both TM and TE field polarization. We consider four different geometries for comparison: the periodic hexagonal pattern with 6-fold symmetry [Fig. 1(a)], and quasicrystalline geometries with 12-fold symmetry (dodecagonal), 8-fold symmetry (octagonal), and 10-fold symmetry (Penrose decagonal), as shown in Figs. 1(b), 1(c), and 1(d) respectively. The PBG

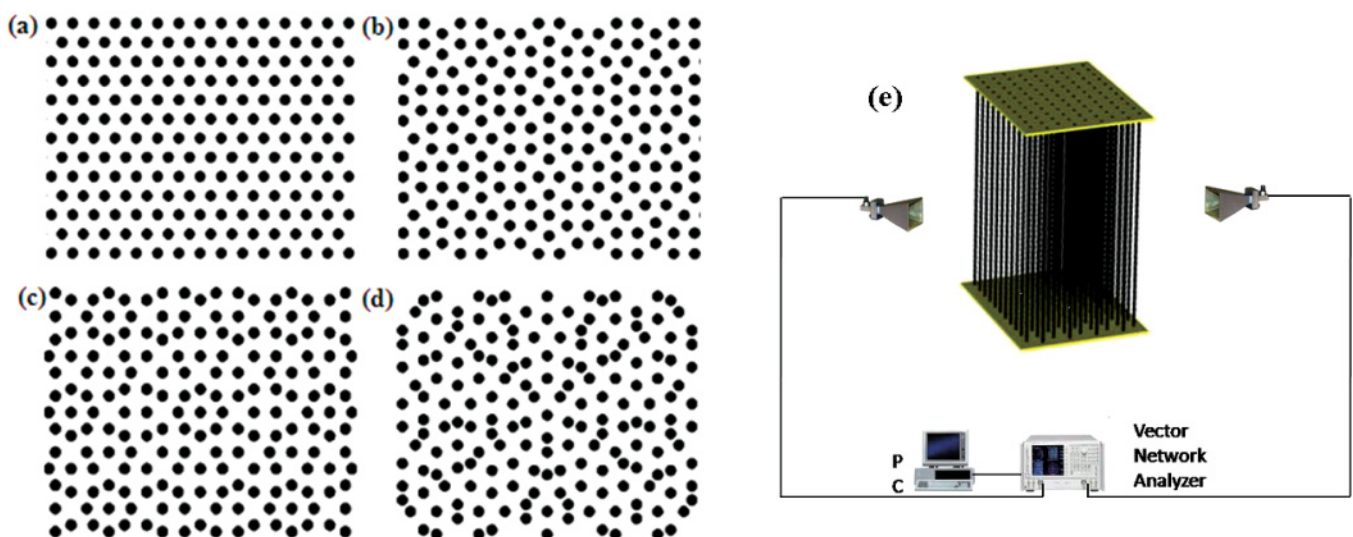


FIG. 1. (Color online) The periodic and aperiodic geometries under study: (a) hexagonal, (b) dodecagonal, (c) octagonal, and (d) decagonal (Penrose). (e) Schematic diagram of the experimental setup (not in scale). Horn antennas are used to transmit and receive the microwave radiation. Data are collected using a vectorial computer-controlled network analyzer. The size of each structure (periodic or aperiodic) is  $0.4 \times 0.14 \times 0.6 \text{ m}^3$ .

properties are studied both numerically and experimentally for two different index contrasts close to the critical values.

## II. COMPUTATIONAL AND EXPERIMENTAL METHODS

The photonic crystals studied consist of infinitely long dielectric cylindrical rods in air placed on the vertices of tiles in the corresponding geometry. The filling factor  $\eta$  is set to be the same for all the structures under study, and is equal to 0.23. The geometries used are shown in Fig. 1. They are designed to have approximately 400 rods in an area of  $\sim 40a \times 14a$ , where  $a$  is a characteristic length of the same order of the tile side length of each structure.

As discussed in the Introduction, from a computational point of view, each quasicrystalline structure presents a challenge in obtaining the information on the photonic band gap since the lack of translational symmetry prevents the rigorous use of the Bloch theorem in the calculations. This difficulty has hampered the use of supercell or similar techniques in the modeling of real aperiodic structure.

The FDTD technique is useful in this respect, since it can provide an alternative, fast, and accurate method to simulate in real space the propagation of the electromagnetic waves through a finite portion of a quasicrystal without resorting to any approximant. A 2D FDTD method with uniaxial perfectly matched layer (PML) boundary conditions (along the  $x$  and  $y$  directions) is employed to obtain transmission characteristics as a function of frequency of the incident radiation, propagation direction, and polarization. In each simulation, the source of excitation consists of a time-pulsed Gaussian beam (with  $250a < b < 800a$ , where  $b$  is the confocal parameter) placed outside the crystal structure and impinging on it with different incidence angles. The field components after propagation through the crystal are collected using a detector (time monitor) placed on the other side of the crystal. The Fourier transform of these data gives the transmission properties as a function of frequency. Both TM and TE polarizations were analyzed in the simulations.

The experiment was designed and carried out in the microwave regime (9–20 GHz). Cross-linked polystyrene (Rexolite) and polytetrafluoroethylene (Teflon) having radius 6.4 mm and length 0.6 m were used to fabricate the cylindrical rods. These materials show a dielectric constant of 2.56 and 2.1, respectively, in the frequency region of interest and a relatively low dissipation. Loss tangent values are in the range between  $10^{-3}$  and  $10^{-4}$ . In order to build up the structure, circular holes with the designed geometries have been drilled onto two support dielectric plates, fixed 0.6 m apart, and then filled with the rods. The characteristic length  $a$  is chosen to be of the order of 1 cm, so that the first PBG appears in the region of 10–12 GHz for all structures under study.

Two high-gain horn antennas acting as a transmitter and a receiver and connected to a two-port vectorial network analyzer (VNA) HP 8720C have been used to obtain the transmission characteristics of the crystals. To change the field polarization, both horn antennas are rotated by  $90^\circ$ . The distance between transmitter and receiver is set to 3 m, so that the polarized signal can be considered a plane wave. In the frequency region of interest, the signal wavelength is much

smaller than the crystal height in the  $z$  direction, therefore one can safely assume that the response has a two-dimensional character in the crystal ( $x$ - $y$ ) plane. Before each measurement, the VNA is calibrated in the absence of the material under study. Transmission curves are then obtained by introducing the sample in between the two horn antennas.

In order to study the isotropic nature of the PBG, the transmission spectra are obtained as a function of incidence angle for all geometries under study. To record the transmission as a function of the direction of propagation of the incident radiation, the crystal is rotated in  $5^\circ$  steps with respect to the normal direction while keeping the position of the antennas unchanged. Because of the  $n$ -fold rotational symmetry of the structures under study, the crystal and quasicrystal properties need only be examined over the  $5^\circ$ – $180^\circ/n$  range since they repeat themselves for any propagation angle outside these degree values. For the sake of clarity, not all angles will be shown in the spectra of the different structures. Measurements were also carried out as a function of crystal thickness for normal transmission only.

## III. RESULTS AND DISCUSSION

The transmission characteristics are measured as a function of incidence angle and compared with simulation results for all geometries under study, using the two materials with different index contrast ( $\Delta n = 0.6$  and  $0.44$  for Rexolite and Teflon, respectively) and for both TM and TE polarization.

Contrary to what happens in the periodic case, defect-free quasiperiodic structures can exhibit localized modes in both stop-band<sup>22,34</sup> and transparency band regions,<sup>35,36</sup> manifesting themselves as relative maxima in the transmission response. Therefore, in analyzing the properties of the quasicrystalline structure, the frequency regions with low transmission are ascribed to PBG effects only (absence of extended modes) rather than light localization (presence of nonextended modes).

### A. Refractive index contrast 0.60

#### 1. TM polarization

Figure 2 shows the experimental and calculated transmission spectra for all the structures under study with an index contrast of 0.60 for various angles of propagation. The experimental results for the hexagonal photonic crystal are presented in Fig. 2(a), whereas Fig. 2(b) shows the corresponding simulation data. In all curves, there is a strong attenuation, from around 30 to 40 dB and more, in the transmission of the electromagnetic waves through the crystal in the region where the first PBG should be present. From the graphs it is clearly observed that the transmission spectra change drastically as the angle of propagation is changed from  $0^\circ$  to  $30^\circ$ . In the case of normal signal incidence ( $0^\circ$ ), the region of low transmission is centered at about 11 GHz and spans  $\sim 2.6$  GHz, with almost no change for an angle  $10^\circ$ . However, as the angle is increased to  $20^\circ$ , changes are clearly visible. The center of this region is shifted to 12 GHz, whereas its width becomes larger ( $\sim 3.3$  GHz). For an angle of  $30^\circ$ , the widening is even stronger. Attenuation increases as the incidence angle does, because of the stronger diffraction that the light undergoes due to the longer path inside the finite crystal. For the first band gap,

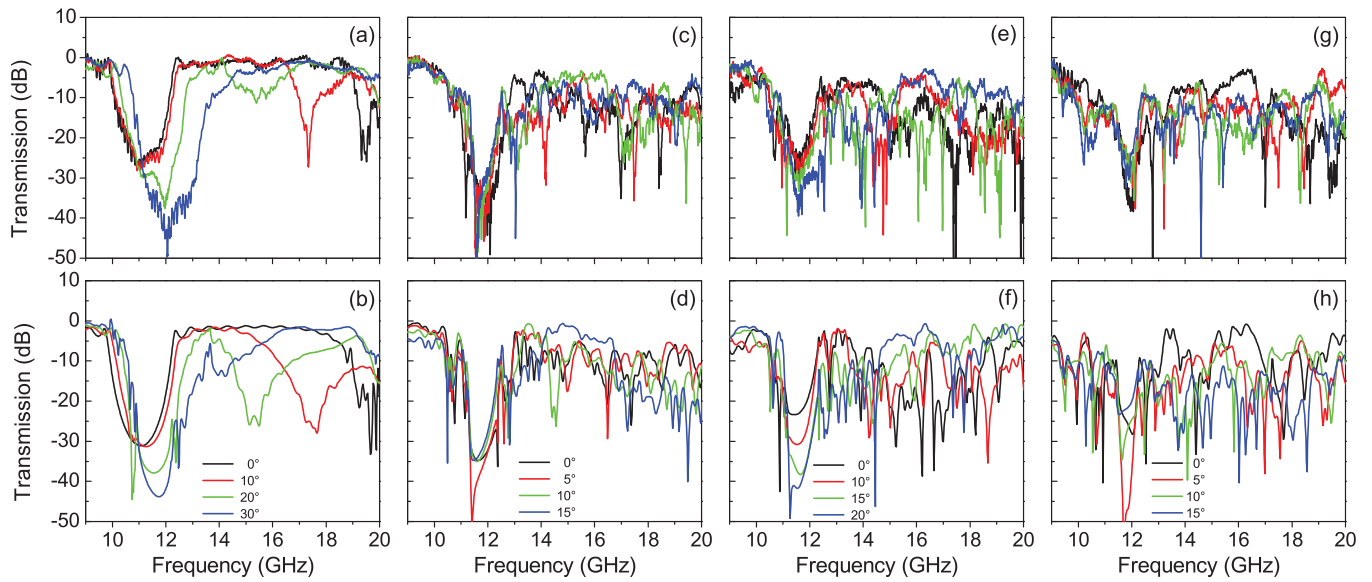


FIG. 2. (Color online) Experimental and calculated transmission spectra of the hexagonal [(a) and (b)], dodecagonal [(c) and (d)], octagonal [(e) and (f)], and decagonal [(g) and (h)] photonic crystals, respectively, for TM polarization. Curves of different colors correspond to different angles of incidence as indicated in the graph.

the experimental results match very well the numerical data reported in Fig. 2(b). At higher frequencies, a second band gap appears with less pronounced characteristics but with a similar angular dependence. Also in this case, there is a fairly good agreement between measurements and simulations.

The transmission characteristics of a dodecagonal PQC structure are shown in Figs. 2(c) and 2(d). A well-pronounced low transmission region, characterized by a signal attenuation larger than 40 dB and extending approximately from 11 to 12.6 GHz, is observed. At higher frequencies, the transmitted power decreases, possibly with the presence of smaller and shallower dips up to the maximum measurement frequency of 20 GHz. The experimental [Fig. 2(c)] and simulation [Fig. 2(d)] angular dependence puts in evidence that in this case, the response is nearly isotropic. Transmission spectra are only slightly affected by the change of the angle of propagation from  $0^\circ$  to  $15^\circ$ .

Similar features are observed for the other aperiodic photonic crystals. In the case of the 8-fold and 10-fold PQC's, the distribution of cylinders has a mirror symmetry with respect to the line of  $22.5^\circ$  and  $18^\circ$ , respectively, and the data are reported in the angular range  $0^\circ$ – $20^\circ$ .

The numerical and experimental results for the case of the octagonal geometry are presented in Figs. 2(e) and 2(f), respectively. The attenuation region is centered at 11.5 GHz for angles from  $0^\circ$  to  $10^\circ$ , whereas it is shifted to  $\sim 11.8$  GHz for incidence at larger angles. There is also a small variation in the width of this region, from 1.4 GHz to  $\sim 2$  GHz.

Data obtained for the Penrose tiled quasicrystal are shown in Figs. 2(g) and 2(h). From both measurements [Fig. 2(g)] and simulations [Fig. 2(h)], one can clearly see that the band gap is not as deep and wide as in the other cases, nevertheless its position and width remain almost the same for all angles.

As in the periodic case, the transmitted signal shows an increasing attenuation region as a function of the incidence angle for all the aperiodic structures. Not surprisingly, the

geometry with 12-fold symmetry is less sensitive to the change in the signal propagation direction. This is likely related to the fact that the band gap for the dodecagonal pattern may be associated with a higher short-range ordering of the dielectric scattering centers in comparison with the other aperiodic structures.<sup>37</sup>

In order to better determine the directional variation of the low transmission region, we measured the upper and lower boundaries as a function of the propagation angle. The region edges are defined as the frequency values for which attenuation reaches 15 dB. Data in Fig. 3 summarize the results found from the observation of the angular dependence. The hexagonal

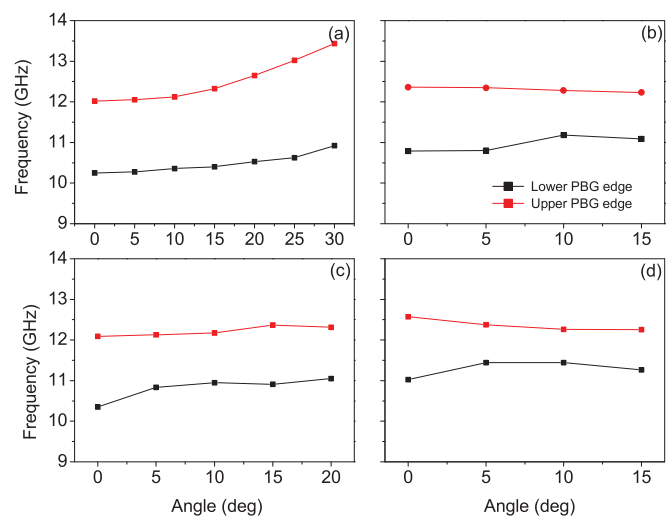


FIG. 3. (Color online) Variation of PBG for TM polarization as a function of angle for the different geometries: (a) hexagonal, (b) dodecagonal, (c) octagonal, and (d) decagonal. In each graph, the black and the red curves indicate the lower and upper frequency edges of the band gap, respectively.

geometry [Fig. 3(a)] clearly shows a strong dependence of the upper and lower frequency edges as a function of angle, whereas its width seems to be less affected. The results for the dodecagonal structure, instead, clearly indicate [see Fig. 3(b)] that its response is highly isotropic, with very small variations of the width and edges at different angles from  $0^\circ$  to  $15^\circ$ . The properties for the octagonal geometry lie somehow in between, since it shows less isotropy compared to the dodecagonal geometry and a noticeable width dependence with respect to the hexagonal case, as displayed in Fig. 3(c) between  $0^\circ$  and  $20^\circ$ . Penrose geometry also seems to have a quite isotropic but narrower low transmission region [Fig. 3(d)] in the same incidence angle range. Considering the omnidirectional response (partial PBG), all the structures under study exhibit a frequency width with similar extension, slightly smaller for the decagonal case only. This low transmission region for aperiodic structures spans from 1.15 GHz (dodecagonal) to 1.05 GHz (octagonal) and 0.8 GHz (Penrose), to be compared with around 1.1 GHz in the case of the periodic crystal.

## 2. TE polarization

The results obtained for the hexagonal and dodecagonal geometries are compared in Fig. 4 for normal incidence only. The hexagonal geometry [Fig. 4(a)] clearly shows a low transmission window  $\sim 1.7$  GHz wide centered at about 11.7 GHz. The experimental (black curve) and calculated (red curve) results are in good agreement. The dodecagonal structure [Fig. 4(b)] displays a very shallow region measured approximately in the region 12–13 GHz (black curve), however only partially reproduced by numerical data (red curve).

Simulation of the response to a TE-polarized wave shows instead that the transmission characteristics for the Penrose and octagonal structures are nearly featureless<sup>31</sup> and are not reported here.

### B. Refractive index contrast 0.44

The results presented in this case are for the hexagonal and dodecagonal cases only. The 8-fold and 10-fold cases were numerically examined in a previous paper,<sup>31</sup> in which we found that these geometries do not show any clear band-gap behavior in the frequency region of interest for index contrast values below 0.6 and for both polarizations.

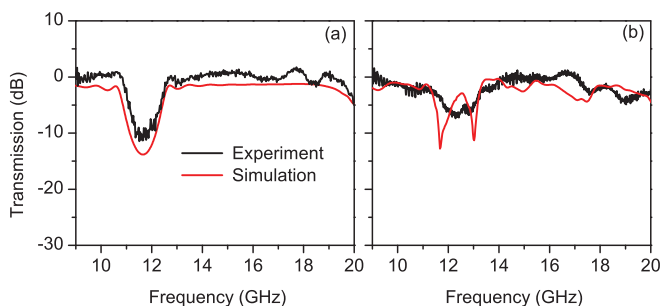


FIG. 4. (Color online) The transmission curves for (a) hexagonal and (b) dodecagonal geometries for normal incidence and TE polarization. Both experimental and simulated results are shown in each graph (red and black curves, respectively).

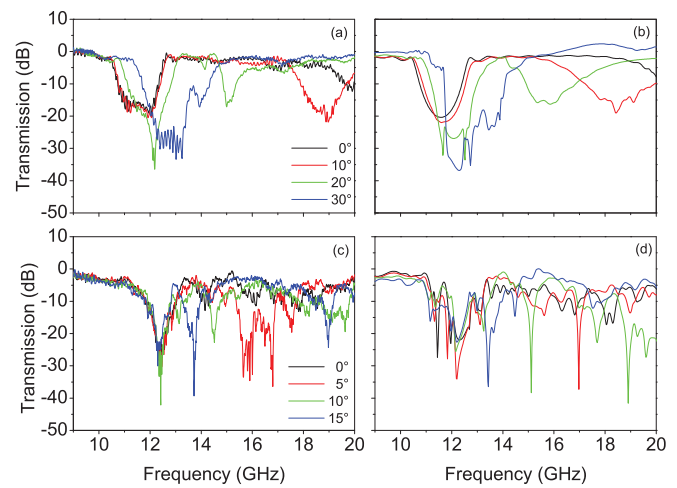


FIG. 5. (Color online) Experimental and calculated transmission spectra of the hexagonal [(a) and (b)] and dodecagonal [(c) and (d)] photonic crystals, respectively, with an index contrast of 0.44 for TM polarization. Curves of different colors correspond to different angles of incidence as indicated in the graph.

For TM polarization, the observed features are similar to the case of the higher refractive index contrast presented above. In this case, the hexagonal crystal shows a strong variation in the attenuation properties as the angle of propagation is varied, as seen in Figs. 5(a) (experiment) and 5(b) (simulation). Similar results for the dodecagonal crystal are presented in Figs. 5(c) and 5(d), respectively. Compared with the case of  $\Delta n = 0.6$ , the width of the low transmission frequency window for a given direction is much narrower for the aperiodic structure than for the periodic one. Nevertheless, the almost negligible angular variation exhibited by the dodecagonal PQC produces a larger partial PBG region. A graph showing the variation of the upper and lower band-edge frequencies as a function of propagation angle is also plotted in Fig. 6 for both the 6-fold and 12-fold symmetry (in the range of  $0^\circ$ – $30^\circ$  and  $0^\circ$ – $15^\circ$ , respectively). As expected due to the lower index contrast, using Teflon cylinders the observed partial PBG's are never as pronounced as in the case of Rexolite, spanning over 300 and 540 MHz for hexagonal and dodecagonal structures, respectively. The nice finding is that the higher isotropy in the response of the PQC almost doubles the value of the observed partial band gap.

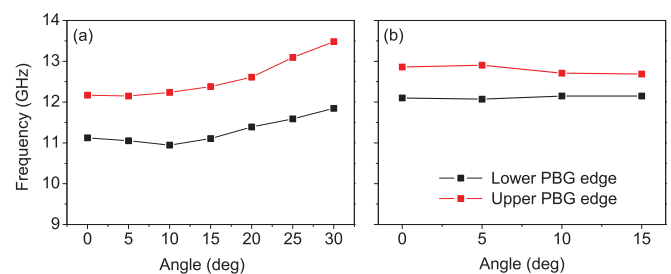


FIG. 6. (Color online) Variation of the low transmission region as a function of angle for (a) hexagonal and (b) dodecagonal geometries, for TM polarization. In each graph, the black and the red curves indicate the lower and upper frequency edges of the band gap, respectively.

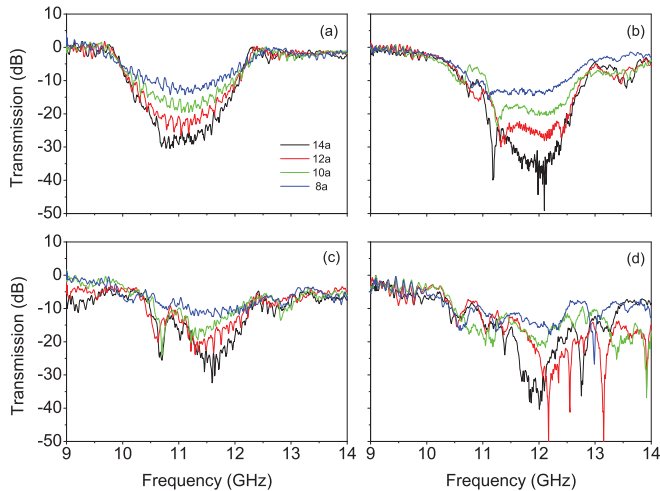


FIG. 7. (Color online) Experimental transmission curves as a function of sample thickness for (a) hexagonal, (b) dodecagonal, (c) octagonal, and (d) decagonal geometries with index contrast 0.60 and TM polarization.

For TE polarization, the features shown in the spectra were so weak that they rendered the study of its angular dependence meaningless. Once again, this is in agreement with the previous simulation work.<sup>31</sup>

### C. Effects of thickness

To understand how sensitive the PBG is to the size of a photonic quasicrystal with a low-index contrast, transmission spectra were also measured by removing the cylinder rows simultaneously from both sides of the structure in the signal propagation direction. Results are shown in Fig. 7 for all aperiodic geometries with an index contrast of 0.6 for normal incidence and in the band-gap region only. The hexagonal case is also reported for comparison. Graphs clearly show that the dodecagonal pattern is less affected by the reduction in size, presenting an appreciable attenuation (15 dB) even when the slab thickness decreases from  $14a$  to  $8a$ . Similar results, but obviously less pronounced, are also obtained for Teflon (10 dB attenuation). This is a further confirmation that the 12-fold geometry is the most robust among the different structures under investigation because of the stronger role played by the short-range interactions, and it is therefore preferable for the development of very compact photonic devices.

## IV. CONCLUSIONS

It is well known<sup>38</sup> that for transverse magnetic modes, band gaps can be easily achieved in photonic crystals made of isolated dielectric rods, whereas connected lattices favor transverse electric gaps. The same happens in photonic quasicrystals, where we have experimentally shown that in the dielectric-in-air configuration, two-dimensional TM band gaps are clearly visible, whereas the response of the aperiodic structures to a TE-polarized signal is very weak or almost featureless. In addition, results were put in evidence that TM band gaps in PQC are possible even with a very low-index contrast, in agreement with numerical studies carried out in Ref. 30. In particular, well-pronounced band gaps are present for the dodecagonal geometry, as theoretically expected because of the higher symmetry.

Also, we did observe that partial band gaps in quasicrystalline geometries are more isotropic than those in periodic crystals, due to their disallowed, noncrystallographic, rotational symmetries. That is, the position and width of the PBG are almost independent of the incident angle of the light, contrary to their periodic counterparts, where gaps of different directions may appear at different frequencies because of the nonspherical first BZ. Using PQC's, therefore, devices exhibiting PBG's with a higher isotropy in comparison with their periodic counterparts can be realized—at little or no expense in terms of size—which can be of interest for specific photonic applications, such as light-emitting diodes or waveguides.

Another important feature of PQC's is that the existence of the gaps is governed by the short-range environment. This is particularly evident in the case of the dodecagonal geometry, where the PBG is robust even for a significant reduction in size in the propagation direction.

In conclusion, this study confirms that quasicrystalline structures having long-range orientational order forbidden for periodic systems are promising candidates as PBG materials. Photonic crystals based on aperiodic specific geometries present extremely interesting features that cannot be achieved in the periodic case. The low-index contrast allows the use of versatile and low-cost technologies such as holographic lithography combined with soft materials for the development of compact devices with switchable properties for an all-optical ultrasmall integrated circuitry.

<sup>1</sup>M. Potter and R. Ziolkowski, *Opt. Express* **10**, 691 (2002).

<sup>2</sup>N. Hitoshi, Y. Sugimoto, K. Kanamoto, N. Ikeda, Y. Tanaka, Y. Nakamura, S. Ohkouchi, Y. Watanabe, K. Inoue, H. Ishikawa, and K. Asakawa, *Opt. Express* **12**, 6606 (2004).

<sup>3</sup>S. H. Fan, P. R. Villeneuve, and J. D. Joannopoulos, *IEEE J. Quantum Electron.* **36**, 1123 (2000).

<sup>4</sup>H. G. Park, J. K. Hwang, J. Huh, H. Y. Ryu, S. H. Kim, J. S. Kim, and Y. H. Lee, *IEEE J. Quantum Electron.* **38**, 1353 (2002).

<sup>5</sup>A. Micco, V. Galdi, F. Capolino, A. Della Villa, V. Pierro, S. Enoch, and G. Tayeb, *Phys. Rev. B* **79**, 075110 (2009).

<sup>6</sup>E. Di Gennaro, C. Miletto, S. Savo, A. Andreone, D. Morello, V. Galdi, G. Castaldi, and V. Pierro, *Phys. Rev. B* **77**, 193104 (2008).

<sup>7</sup>E. Di Gennaro, S. Savo, A. Andreone, V. Galdi, G. Castaldi, V. Pierro, and M. R. Masullo, *Appl. Phys. Lett.* **93**, 164102 (2008).

<sup>8</sup>C. Sibilia, I. S. Nefedov, M. Scalora, and M. Bertolotti, *J. Opt. Soc. Am. B* **15**, 1947 (1998).

<sup>9</sup>M. A. Kaliteevski, S. Brand, R. A. Abram, T. F. Krauss, R. M. de la Rue, and P. Millar, *J. Mod. Opt.* **47**, 1771 (2000).

- <sup>10</sup>M. A. Kaliteevski, S. Brand, R. A. Abram, T. F. Krauss, R. DeLa Rue, and P. Millar, *Nanotechnology* **11**, 274 (2000).
- <sup>11</sup>X. D. Zhang, Z. Q. Zhang, and C. T. Chan, *Phys. Rev. B* **63**, 081105 (2001).
- <sup>12</sup>C. J. Jin, B. Y. Cheng, B. Y. Man, Z. L. Li, D. Z. Zhang, S. Z. Ban, and B. Sun, *Appl. Phys. Lett.* **75**, 1848 (1999).
- <sup>13</sup>A. Della Villa, S. Enoch, G. Tayeb, V. Pierro, V. Galdi, and F. Capolino, *Phys. Rev. Lett.* **94**, 183903 (2005).
- <sup>14</sup>M. Notomi, H. Suzuki, T. Tamamura, and K. Edagawa, *Phys. Rev. Lett.* **92**, 123906 (2004).
- <sup>15</sup>M. E. Zoorob, M. D. B. Charlton, G. J. Parker, J. J. Baumberg, and M. C. Netti, *Nature (London)* **404**, 740 (2000).
- <sup>16</sup>J. Lourtioz, H. Benisty, V. Berger, J. Gerard, D. Maystre, and A. Tchebnokov, *Photonic Crystals* (Springer, Berlin, 2008).
- <sup>17</sup>A. W. Rodriguez, A. P. McCauley, Y. Avniel, and S. G. Johnson, *Phys. Rev. B* **77**, 104201 (2008).
- <sup>18</sup>W. Steurer and D. Sutter-Widmer, *J. Phys. D* **40**, R229 (2007).
- <sup>19</sup>J. E. S. Socolar, *Phys. Rev. B* **39**, 10519 (1989).
- <sup>20</sup>R. Penrose, *Bull. Inst. Math. Appl.* **10**, 266 (1974).
- <sup>21</sup>P. Stampfli, *Helv. Phys. Acta* **59**, 1260 (1986).
- <sup>22</sup>X. Wang, C. Y. Ng, W. Y. Tam, C. T. Chan, and P. Sheng, *Adv. Mater.* **15**, 1526 (2003).
- <sup>23</sup>R. Gauthier and K. Mnaymneh, *Opt. Express* **13**, 1985 (2005).
- <sup>24</sup>G. Zito, B. Piccirillo, E. Santamato, A. Marino, V. Tkachenko, and G. Abbate, *Opt. Express* **16**, 5164 (2008).
- <sup>25</sup>A. Harb, F. Torres, K. Ohlinger, Y. K. Lin, K. Lozano, D. Xu, and K. P. Chen, *Opt. Express* **18**, 011110 (2010).
- <sup>26</sup>S. P. Gorkhali, J. Qi, and G. P. Crawford, *Appl. Phys. Lett.* **86**, 20512 (2005).
- <sup>27</sup>M. Florescu, S. Torquato, and P. J. Steinhardt, *Phys. Rev. B* **80**, 155112 (2009).
- <sup>28</sup>The index contrast is defined in the following simply as the difference between the refractive indexes of the dielectric material and air.
- <sup>29</sup>A. Matthews, X. H. Wang, Y. Kivshar, and M. Gu, *Appl. Phys. B* **81**, 189 (2005).
- <sup>30</sup>M. C. Rechtsman, H. C. Jeong, P. M. Chaikin, S. Torquato, and P. J. Steinhardt, *Phys. Rev. Lett.* **101**, 073902 (2008).
- <sup>31</sup>G. Zito, T. P. Rose, E. Di Gennaro, A. Andreone, E. Santamato, and G. Abbate, *Microwave Opt. Technol. Lett.* **51**, 2732 (2009).
- <sup>32</sup>M. Bayindir, E. Cubukcu, I. Bulu, and E. Ozbay, *Phys. Rev. B* **63**, 161104 (2001).
- <sup>33</sup>M. Hase, H. Miyazaki, M. Egashira, N. Shinya, K. M. Kojima, and S. I. Uchida, *Phys. Rev. B* **66**, 214205 (2002).
- <sup>34</sup>K. Mnaymneh and R. C. Gauthier, *Opt. Express* **15**, 5089 (2007).
- <sup>35</sup>A. Della Villa, S. Enoch, G. Tayeb, F. Capolino, V. Pierro, and V. Galdi, *Opt. Express* **14**, 10021 (2006).
- <sup>36</sup>Y. Neve-Oz, T. Pollok, S. Burger, M. Golosovsky, R. Lifshitz, and D. Davidov, *International Conference of Numerical Analysis and Applied Mathematics*, edited by T. E. Simos, G. Psihoyios, Ch. Tsitouras, AIP Conf. Proc. No. 1281 (AIP, New York, 2010), p. 1622.
- <sup>37</sup>Y. S. Chan, C. T. Chan, and Z. Y. Liu, *Phys. Rev. Lett.* **80**, 956 (1998).
- <sup>38</sup>J. D. Joannopoulos, R. D. Meade, and J. N. Winn, *Photonic Crystals: Molding the Flow of Light* (Princeton University Press, Princeton, NJ, 1995).